

Lrig2 and Hpse2, mutated in urofacial syndrome, pattern nerves in the urinary bladder



OPEN

Neil A. Roberts¹, Emma N. Hilton¹, Filipa M. Lopes¹, Subir Singh¹, Michael J. Randles², Natalie J. Gardiner³, Karl Chopra¹, Riccardo Coletta^{1,4}, Zunera Bajwa¹, Robert J. Hall^{5,6}, Wyatt W. Yue⁷, Franz Schaefer⁸, Stefanie Weber⁹, Roger Henriksson^{10,11}, Helen M. Stuart^{5,6}, Håkan Hedman¹⁰, William G. Newman^{5,6} and Adrian S. Woolf^{1,4}

¹Division of Cell Matrix Biology and Regenerative Medicine, School of Biological Sciences, Faculty of Biology Medicine and Health, University of Manchester, UK; ²School of Allied Health Sciences, De Montfort University, Leicester, UK; ³Division of Diabetes, Endocrinology and Gastroenterology, School of Medical Sciences, Faculty of Biology, Medicine and Health, University of Manchester, Manchester, UK; ⁴Royal Manchester Children's Hospital, Manchester University NHS Foundation Trust, Manchester Academic Health Science Centre, Manchester, UK; ⁵Division of Evolution and Genomic Sciences, School of Biological Sciences, Faculty of Biology, Medicine and Health, University of Manchester, UK; ⁶Manchester Centre for Genomic Medicine, St. Mary's Hospital, Manchester University NHS Foundation Trust, Manchester Academic Health Science Centre, Manchester, UK; ⁷Structural Genomics Consortium, Nuffield Department of Clinical Medicine, University of Oxford, UK; ⁸Division of Pediatric Nephrology, Centre for Pediatric and Adolescent Medicine, University Hospital of Heidelberg, Im Neuenheimer Feld, Heidelberg, Germany; ⁹Pediatric Nephrology, University-Children's Hospital Marburg, Philipps-University Marburg, Germany; ¹⁰Department of Radiation Sciences, Oncology, Umeå University, Umeå, Sweden; and ¹¹Regional Cancer Center Stockholm/Gotland, Stockholm, Sweden

Mutations in leucine-rich-repeats and immunoglobulin-like-domains 2 (LRIG2) or in heparanase 2 (HPSE2) cause urofacial syndrome, a devastating autosomal recessive disease of functional bladder outlet obstruction. It has been speculated that urofacial syndrome has a neural basis, but it is unknown whether defects in urinary bladder innervation are present. We hypothesized that urofacial syndrome features a peripheral neuropathy of the bladder. Mice with homozygous targeted *Lrig2* mutations had urinary defects resembling those found in urofacial syndrome. There was no anatomical blockage of the outflow tract, consistent with a functional bladder outlet obstruction. Transcriptome analysis revealed differential expression of 12 known transcripts in addition to *Lrig2*, including 8 with established roles in neurobiology. Mice with homozygous mutations in either *Lrig2* or *Hpse2* had increased nerve density within the body of the urinary bladder and decreased nerve density around the urinary outflow tract. In a sample of 155 children with chronic kidney disease and urinary symptoms, we discovered novel homozygous missense *LRIG2* variants that were predicted to be pathogenic in 2 individuals with non-syndromic bladder outlet obstruction. These observations provide evidence that a peripheral neuropathy is central to the pathobiology of functional bladder outlet obstruction in urofacial syndrome, and emphasize the importance of *LRIG2* and *heparanase 2* for nerve patterning in the urinary tract.

Kidney International (2019) **95**, 1138–1152; <https://doi.org/10.1016/j.kint.2018.11.040>

KEYWORDS: autonomic; ganglia; gene; mouse; urination

Copyright © 2019, International Society of Nephrology. Published by Elsevier Inc. This is an open access article under the CC BY-NC-ND license (<http://creativecommons.org/licenses/by-nc-nd/4.0/>).

Translational Statement

These observations collectively provide evidence that a peripheral neuropathy is central to the pathobiology of urofacial syndrome bladder disease and emphasize the importance of leucine-rich repeats and Ig-like domains 2 and heparanase 2 in the urinary tract. Further definition of the molecular pathobiology underlying urofacial syndrome may reveal new therapeutic targets in bladder dysfunction. Gene therapy is now being used for certain rare genetic diseases. The encouraging clinical outcomes of babies with spinal muscular atrophy treated with adeno-associated virus-mediated replacement of a missing molecule¹ could serve as a paradigm for congenital diseases of the urinary tract, such as urofacial syndrome. Here, a next step will be to test adeno-associated virus-mediated gene therapy in *heparanase 2* and *leucine-rich repeats and Ig-like domains 2* mutant mouse models of urofacial syndrome.

Correspondence: Neil A. Roberts, Michael Smith Building, University of Manchester, Oxford Road, Manchester M13 9PT, UK. E-mail: neil.roberts-2@manchester.ac.uk

Received 19 July 2018; revised 6 November 2018; accepted 21 November 2018; published online 8 March 2019

Bladders undergo filling and voiding cycles controlled by autonomic nerves.^{2,3} Preganglionic autonomic neurons have cell bodies in the spinal cord, and their axons synapse within ganglia with postganglionic neurons whose axons innervate bladder muscles. Sympathetic noradrenergic neurons elicit outflow tract contraction during urinary storage, whereas during voiding, parasympathetic cholinergic

motor neurons drive detrusor smooth muscle contraction and neuronal nitric oxide synthase (nNOS)-expressing neurons dilate the outflow tract.⁴ Urofacial, or Ochoa, syndrome (UFS) is an autosomal-recessive disease with around 150 families reported worldwide.^{5,6} In persons with UFS, detrusor smooth muscle contracts against a poorly dilated outflow tract, causing functional bladder outlet obstruction.^{5,6} This dyssynergia causes dribbling incontinence and residual urine, leading to a risk of ascending bacterial infection and kidney failure. The UFS bladder is a “non-neurogenic neurogenic bladder” resembling that caused by damaged bladder nerves, yet such gross lesions are absent in persons with UFS.^{5,6} Persons with UFS typically have a facial expression “as if in pain or sadness when they tried to smile or laugh.”⁵ Ochoa,⁵ who first delineated the syndrome, and others⁷ speculated that there is a neuropathic basis for UFS.

Some families with UFS have biallelic variants in *heparanase 2* (*HPSE2*)^{8–10} encoding heparanase 2, an inhibitor of the enzyme activity of the classical heparanase protein,¹¹ hereafter called “heparanase.” Homozygous *Hpse2* gene-trap mice have incomplete bladder emptying,^{10,12} phenocopying UFS. Whether *Hpse2* mutant mouse bladders have innervation defects is unknown. Other families with UFS lack *HPSE2* mutations; some instead have biallelic variants of leucine-rich repeats and Ig-like domains 2 (*LRIG2*).^{13,14} The most studied of the 3 mammalian *Lrig* proteins is *Lrig1*, a tumor suppressor that downregulates growth factor signaling.^{15–17} Belonging to the family of leucine-rich repeat-containing proteins, *LRIG2* comprises multiple leucine-rich repeats, 3 Ig-like domains, a transmembrane segment, and a long cytosolic portion.¹⁸ Homozygous *Lrig2* mutant mice are protected from growth factor-induced gliomas, but their bladders were not studied.¹⁹

Because heparanase 2 and *Lrig2* are immunodetected in fetal mouse¹⁰ and human¹³ bladder nerves, these proteins are well placed to affect nerve patterning. We hypothesized that UFS features a peripheral neuropathy of the bladder. We studied gene-targeted *Lrig2* mice, demonstrating that they have defective urination and abnormal patterns of bladder nerves. We went on to show that *Hpse2* mutant mice have similar defects. To date, only a few families with *LRIG2* mutations have been reported.^{13,14} Accordingly, we studied persons with nonsyndromic bladder outlet obstruction and report homozygous *LRIG2* likely pathogenic missense variants in a subset.

RESULTS

Lrig2 mutant mice have abnormal urination

We used mice with a targeted deletion of *Lrig2* exon 12,¹⁹ which introduces a frameshift preceding the region encoding the transmembrane domain, generating multiple stop codons. Mice had been maintained on a C57BL/6 background for more than 10 generations, and mating heterozygotes generated offspring for study. Upon analyzing the bladder and outflow tract unit, quantitative reverse transcription-polymerase chain reaction

(qRT-PCR) detected *Lrig2* in wild-type neonatal (first postnatal day) samples. In *Lrig2*^{−/−} littermates, transcripts were undetectable using exon 12 primers and were significantly diminished ($P = 0.0163$) to one third of wild-type levels using exon 17 primers (Figure 1a). Using an antibody to a cytosolic *Lrig2* epitope absent in *Lrig1* and *Lrig3*,¹⁹ *Lrig2* was detected as a 125-kDa band in Western blots of wild-type bladders (Figure 1b). *Lrig2* was absent in *Lrig2*^{−/−} littermates, with intermediate levels in *Lrig2*^{+/-} samples (Figure 1b and c). Neonatal mice of the 3 genotypes had similar weights. At 2 weeks, *Lrig2*^{−/−} mice had gained less weight than the other genotypes, being on average 14% lighter than *Lrig2*^{+/+} or *Lrig2*^{+/-} littermates. Neonatal necropsy bladders, examined within 5 minutes of cervical dislocation, were classified as empty or containing urine by visual inspection. Approximately 90% of bladders contained urine in all 3 genotypes (Figure 1d). At 2 weeks (Figure 1e), 67% of *Lrig2*^{−/−} mouse bladders contained urine, a significant ($P = 0.014$) increase versus 21% of wild-type bladders. The frequency of heterozygous bladders containing urine was similar to wild types. These and adult mice were studied by the voided stain on paper (VSOP) technique²⁰ where they urinate onto filter paper, with numbers and sizes of spots measured. Wild-type and heterozygous *Lrig2* mice voided once or twice per hour, whereas homozygous *Lrig2* mutant mice voided up to 20 times per hour, producing smaller spots than *Lrig2*^{+/+} or *Lrig2*^{+/-} mice (Figure 1f). Quantification (Figure 1g) showed that *Lrig2*^{−/−} mice voided more frequently ($P = 0.001$), and their average volume per void was lower ($P = 0.0124$) compared with control subjects. Total urine voided per time was similar in control (*Lrig2*^{+/+} and *Lrig2*^{+/-}) mice and *Lrig2*^{−/−} mice. These aberrant urination patterns, observed from 14 days to adulthood, resemble those in UFS.^{5,6} UFS uropathy is not sex limited,⁵ and both male and female *Lrig2*^{−/−} mice had abnormal urination. Ink was injected into the bladder lumen at autopsy, and upon gentle palpation, ink exited the urethra. Upon histologic examination (Supplementary Figure S1A–F), bladder outflows were patent in neonatal, juvenile, and adult *Lrig2*^{−/−} mice. Histology of the bladder body was similar in wild types and mutants at 2 weeks (Supplementary Figure S1G–L). Adult *Lrig2*^{−/−} bladders appeared larger than wild types (Figure 2a). Histology with picrosirius red, a collagen reactive dye, revealed prominent staining in mutant lamina propria and detrusor (Figure 2b and c). *Lrig2*^{−/−} kidneys showed no scarring (Figure 2d and e). After draining urine from bladders, mutant organs were significantly heavier than those of control subjects (Figure 2f). Immunostaining adult bladders for Ki67 (Supplementary Figure S2) revealed similar proportions of proliferating nuclei in mutants and control subjects (Figure 2g–i). Detrusor nuclei number was similar ($P = 0.36$) in control mice (mean \pm SEM, $431 \pm 88/\text{mm}^2$, $n = 4$) and mutants ($453 \pm 53/\text{mm}^2$, $n = 4$).

Transcriptome analyses of *Lrig2* mutants

To investigate the molecular milieu before urination defects became established, we undertook RNA sequencing of neonatal bladders and their attached outflow tracts harvested

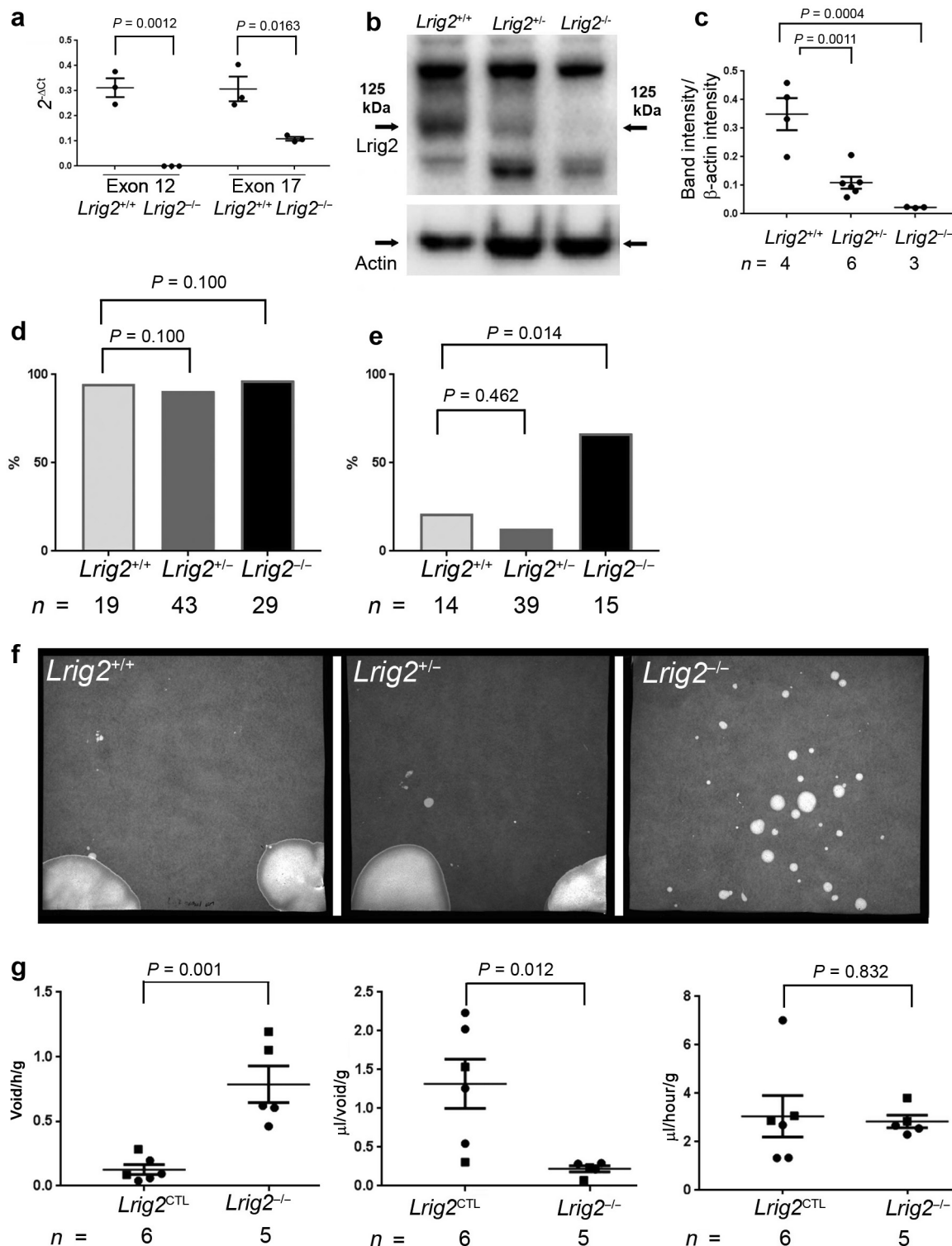


Figure 1 | Leucine-rich repeats and Ig-like domains 2 (*Lrig2*) expression and urination patterns in mice. (a) Quantitative reverse transcription–polymerase chain reaction demonstrated that *Lrig2* transcripts were present in wild-type bladders. In tissues from *Lrig2*^{-/-} littermates, transcripts were undetectable using exon 12 primers ($P = 0.0012$, 2-tailed unpaired Student *t*-test), and there were diminished levels of transcripts in *Lrig2*^{-/-} versus *Lrig2*^{+/+} tissues as assessed by exon 17 primers ($P = 0.0163$, 2-tailed unpaired Student *t*-test, $n = 4$). (b) Western blotting indicated that *Lrig2*, the 125-kDa band, was present in wild-type and heterozygous bladders but was not detected in homozygous mutant tissues. The panel below shows lysates from the same 3 organs probed for the housekeeping protein, β -actin (Actin). (c) Semiquantification of Western blot signals showed diminished values in both *Lrig2*^{+/-} ($P = 0.0011$) and *Lrig2*^{-/-} ($P = 0.0004$) tissues compared with wild types (ordinary one-way analysis of variance with Tukey's multiple comparisons test). In (a) and (c), error bars are SEM. (d) Frequency of necropsy bladders containing urine in neonatal mice. Bladders from wild-type, heterozygous, and (continued)

from 5 *Lrig2*^{+/+} and *Lrig2*^{-/-} littermate pairs. We used females because the male tract includes the prostatic rudiment, with a transcriptome that could complicate interpretation of resulting arrays. The data set is available from *ArrayExpress* (E-MTAB-6089). Unsupervised hierarchical clustering distinguished between homozygous *Lrig2* mutants and wild types (Figure 3a). Thirteen significantly differentially regulated known transcripts were identified after adjusting for multiple comparisons. As expected, *Lrig2* was one of the downregulated transcripts. Gene ontology analysis (Figure 3b) revealed enrichment of cell differentiation and system development terms. The only tissue-specific enriched term was nervous system development. Several of these transcripts encode proteins implicated in neurobiology, as detailed in the Discussion section.

UFS proteins in bladder nerves

The RNA sequencing results were generally consistent with the hypothesis that the UFS bladder has a neural component, and this led us to examine nerve patterns in *Lrig2*^{-/-} bladders. In mice, the 2 pelvic ganglia flank the bladder outflow.^{3,21} We studied wild-type mice two thirds through gestation, when these ganglia are composed of loose aggregates¹⁰ of neural crest-derived cells²² and the bladder rudiment has acquired well-defined body and outflow tract. *Lrig2* *in situ* hybridization demonstrated prominent signals at the junction of the body and outflow tract (Figure 4a), the sites of pelvic ganglia immunostaining for peripherin, a neural intermediate filament (Figure 4b). Embryonic pelvic ganglia were explanted and cultured, adapting published protocols.^{23,24} During the next day, processes and cell bodies emanated from cell aggregates (Figure 4c). The processes immunostained for the neuronal microtubule protein β 3-tubulin (Figure 4d) and migrating cell bodies immunostained for S100B, a calcium-binding protein expressed by autonomic ganglia glia.²⁵ *Lrig2* was immunodetected in cell bodies within explanted aggregates; it was immunodetected faintly in the emerged neurites and more prominently in emerged glia-like cells (Figure 4e). Heparanase 2 was immunodetected in cell bodies, neurites, and glia-like cells (Figure 4f). Heparanase, the classical heparanase,¹¹ was immunodetected in neurite-like structures (Figure 4g). Upon histologic examination, pelvic ganglia of neonatal wild-type mice immunostained for *Lrig2*, heparanase 2, and heparanase (Figure 4h). Immunohistochemistry for *Wnt4* and *Capza1*, encoded by 2 transcripts highlighted in unsupervised hierarchical clustering (Figure 3),

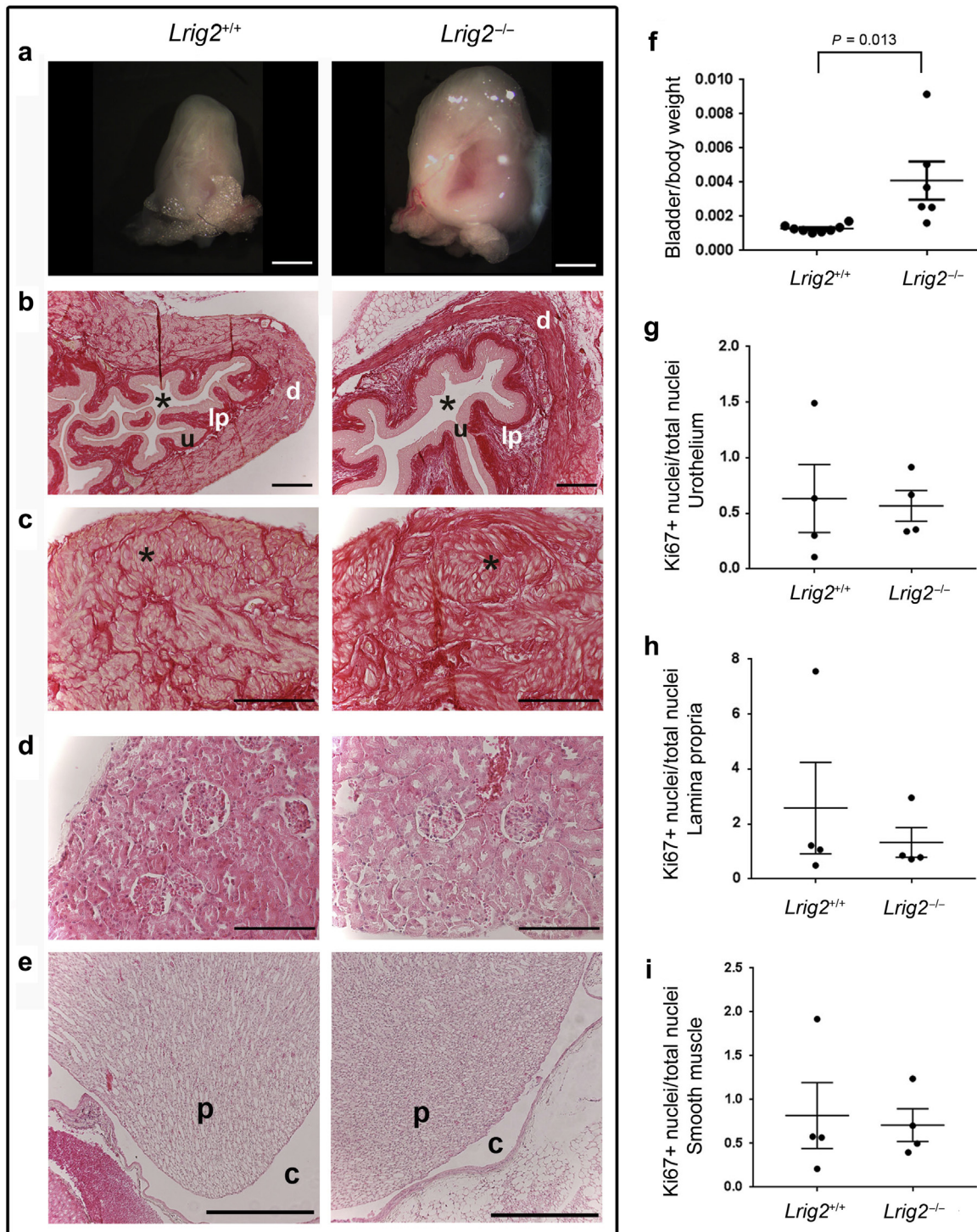
showed that they were detectable in neonatal pelvic ganglia (Supplementary Figure S3). In wild-type neonatal ganglia, 9% of nuclei were Ki67⁺. Pelvic ganglia in *Lrig2*^{-/-} littermates had a similar ($P = 0.190$) proportion of positive nuclei ($n = 4$ mice, each genotype).

Aberrant patterns of nerves in bladders of mice mutant for *Lrig2* or *Hpse2*

Bladders harvested from mice in the second week after birth were cut open, generating butterfly shaped sheets, and whole-mount immunostained for peripherin. In *Lrig2* mutant and wild-type littermate bladders, pelvic ganglia expressed peripherin, as did nerves at the junction of the outflow and the bladder base and nerves in the body (Figure 5). Representative bladders are shown in increasing magnifications in Figure 5a, b, and c. We noted 2 characteristic changes in mutants versus wild types. First, large nerve bundles in the bladder base (black asterisks, Figure 5a) continuous with the pelvic ganglia appeared to be less compactly bundled. Second, there appeared to be an increased density of smaller nerves in the bladder body (Figure 5b and c). Upon quantification by observers blinded to genotypes, a significant ($P = 0.048$) increase of peripherin+ structures was confirmed in *Lrig2* mutant bladders (Figure 5d). Using VSOP analyses (Figure 6a), *Hpse2* homozygous gene-trap mice¹⁰ produced significantly more voids per unit time ($P = 0.003$) than did control (wild-type and heterozygous) littermates (Figure 6b). Mutant void volumes were significantly ($P = 0.012$) smaller than those of control mice (Figure 6c), but with no significant difference ($P = 0.423$) in total volumes urinated per unit time (Figure 6d). These aberrant urination patterns resemble those reported in another *Hpse2* gene trap mouse.¹² Bladder sheet immunostaining demonstrated bundles of peripherin+ nerves in bladder body that appeared more prominent in *Hpse2* mutants than in control bladders (Figure 6e). Quantification showed an increase ($P = 0.004$) of peripherin+ structures in *Hpse2*^{-/-} versus *Hpse2*^{+/+} littermates (Figure 6f). *Hpse2* and *Lrig2* lines were interbred, generating transheterozygotes—that is, mice carrying one mutant allele at each locus. Upon being studied by VSOP ($n = 6$ adults, a cohort containing males and females), their urination patterns appeared similar to wild-type or single heterozygous littermates.

Nerves around the outflow tract were analyzed in the second week after birth (Figure 7a). In wild types, peripherin immunostaining revealed ganglia flanking the outflow tract, with prominent nerve bundles between them, lying in the

Figure 1 | (continued) homozygous mice nearly always contained urine ($P = 0.100$, Fisher exact test). (e) Frequency of bladders containing urine at necropsy at 2 weeks after birth. *Lrig2*^{-/-} bladders contained urine significantly more often than did wild types ($P = 0.014$, Fisher exact test), whereas heterozygous bladders were similar to wild types ($P = 0.462$, Fisher exact test). (f) Urination patterns in weaned mice as assessed by voided stain on paper. The wild-type and heterozygous mice produced a few large voids in the observation period, whereas the *Lrig2*^{-/-} mouse produced many smaller voids in the same period. (g) Left panel: numbers of voids per unit time, with a significant increase in homozygous mutants versus control subjects ($P = 0.001$). Middle panel: volumes of urine per void, with a significant decrease in homozygous mutants versus control subjects ($P = 0.012$). Right panel: total volumes of urine produced per unit time, with no significant difference ($P = 0.832$) between control (comprising wild-type and heterozygous mice) and *Lrig2*^{-/-} littermates. Data are mean \pm SEM, with values factored for weights of individual mice, with comparisons using 2-tailed unpaired Student *t*-test. Note that increased frequency of urination was observed in both male (boxes) and female (circles) homozygous mutant mice. To optimize viewing of this image, please see the online version of this article at www.kidney-international.org.



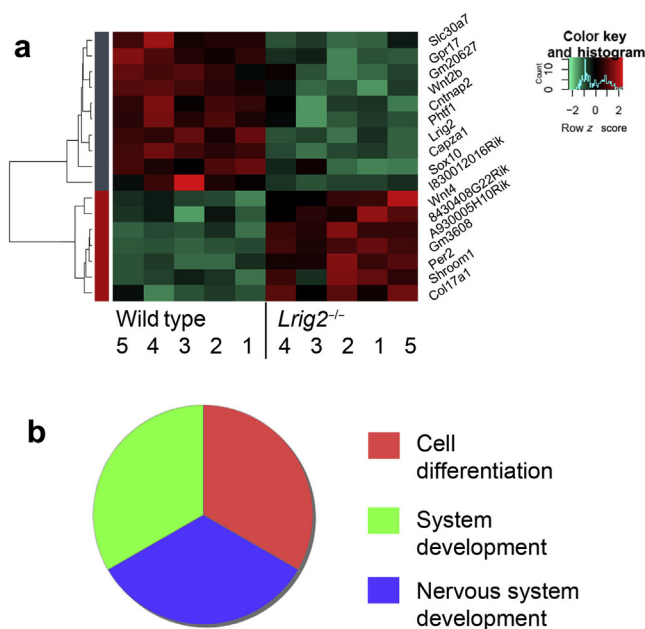


Figure 3 | RNA sequencing analyses. (a) Unsupervised hierarchical clustering distinguished between wild-type ($n = 5$) and homozygous *Leucine-rich repeats* and *Ig-like domains 2* (*Lrig2*)^{-/-} ($n = 5$) bladders and their attached outflow tracts. Rows are expression levels denoted as the z score, displayed in a high–low (red–green) color scale. (b) Gene ontology analysis using the Panther Classification System. The only tissue-specific enriched term was *nerve system development*.

dorsal side of the outflow. In *Lrig2* or *Hpse2* homozygous mutants, a spectrum of aberrations was observed, from disorganized to almost absent peripherin+ nerves. Next, we used markers of specific neural subtypes: anti-nNOS immunostaining to detect nitrergic parasympathetic nerves and anti-tyrosine hydroxylase immunostaining to mark sympathetic nerves. In control subjects, a subset of cell bodies in pelvic ganglia were nNOS⁺, and fine bundles connecting the pelvic ganglia were also nNOS⁺. nNOS⁺ cell bodies also were observed in ganglia of *Lrig2*^{-/-} or *Hpse2*^{-/-} bladders. In contrast, patterns of nNOS⁺ connecting nerves appeared aberrant in either mutant, sometimes with barely any positive processes detected. In wild-type outflow tracts, anti-tyrosine hydroxylase immunostaining was detected in a subset of cell bodies in ganglia and in nerve bundles spanning pelvic ganglia. In mutant outflow tracts, anti-tyrosine hydroxylase immunostaining+ bundles appeared disorganized or reduced. Numbers of peripherin-positive nerves around outflow tracts (Figure 7b) were significantly less in either *Lrig2* or *Hpse2* homozygous mutants compared with control mice. In histologic sections of neonatal bladders, nNOS was immunodetected in pelvic ganglia (Supplementary Figure S3), with a small but statistically significant reduction of signal intensity in *Lrig2*^{-/-} ganglia. qRT-PCR for *Nos1* in neonatal bladders and outflow tracts showed significantly reduced levels in *Lrig2* and *Hpse2* mutants (Supplementary Figure S4). This finding was consistent with the RNA sequencing, which revealed that *Lrig*^{-/-} mutant bladders had average *Nos1* levels of 48% of

wild-type values ($P = 0.001$, when multiple comparison testing was not used). Numbers of processes emanated from explanted pelvic ganglia fragments were similar in mutants and control subjects (Supplementary Figure S5).

***LRIG2* variants in nonsyndromic bladder outlet obstruction**

Putative loss-of-function *LRIG2* variants have been described in UFS.¹³ We also reported compound heterozygous missense *LRIG2* variants (p.Arg550Cys in exon 13 and p.Ile852Phe in exon 16) in a patient with a non-neurogenic neurogenic bladder but with a normal smile.¹³ To seek *LRIG2* variants in other uropathies, we used Sanger sequencing for *LRIG2* in children with chronic kidney failure from the 4C Study (<http://www.4c-study.org/>). We focused on a subset of 155 patients with urinary tract symptoms (e.g., incontinence of urine and poor stream) and/or signs (e.g., abnormal urinary tract radiology). Two individuals were found to have homozygous missense variants in *LRIG2*. One harbored c.1337T>C; p.(Leu446Pro) in exon 12, absent in control databases including >120,000 persons in the Genome Aggregation Database (<http://gnomad.broadinstitute.org>) and predicted to be deleterious by *in silico* tools including Sorting Intolerant From Tolerant, Polymorphism Phenotyping version 2), and MutationTaster. This individual had a non-neurogenic neurogenic bladder but lacked UFS facial features. Another patient harbored c.1948C>T; p.(Arg650Cys) in exon 14 of *LRIG2*. This characteristic has been reported in 8 of 277158 alleles in the Genome Aggregation Database but never in the homozygous state and is predicted to be deleterious by Sorting Intolerant From Tolerant, Polymorphism Phenotyping version 2, and MutationTaster. The patient had congenital bladder outlet obstruction but lacked UFS facial features. It was not possible to obtain to access relatives. The 2 cases were Turkish, so we screened 85 healthy Turkish control subjects but failed to find either Leu446Pro or Arg650Cys variants in 170 chromosomes. Figure 8a shows that both Leu446 and Arg650 are conserved between human, mouse, chicken, xenopus, and zebrafish protein sequences. As detailed in the Supplementary Results text and depicted in Figure 8b–d, these missense *LRIG2* variants may have an impact on the structural integrity of the *LRIG2* extracellular region by affecting disulphide bonds for Leu446Pro and a salt bridge for Arg650Cys. *LRIG2* exons 12, 13, 14, and 16, known to harbor missense variants in non-neurogenic neurogenic bladder, were sequenced in 192 index cases from the United Kingdom Vesicoureteric Reflux (VUR) DNA Collection.²⁶ They had familial primary nonsyndromic VUR, ureter malformations without anatomic bladder outlet obstruction, non-neurogenic neurogenic bladder, or extrarenal malformations. Five rare heterozygous *LRIG2* variants were identified in index cases, but no biallelic variants were detected. Only 2 variants segregated with disease and neither was uniformly predicted.

DISCUSSION

In rats, neuromuscular functional maturation of detrusor smooth muscle occurs in the few first weeks after birth.²⁷ Our results show that bladders in newborn mice, whether wild

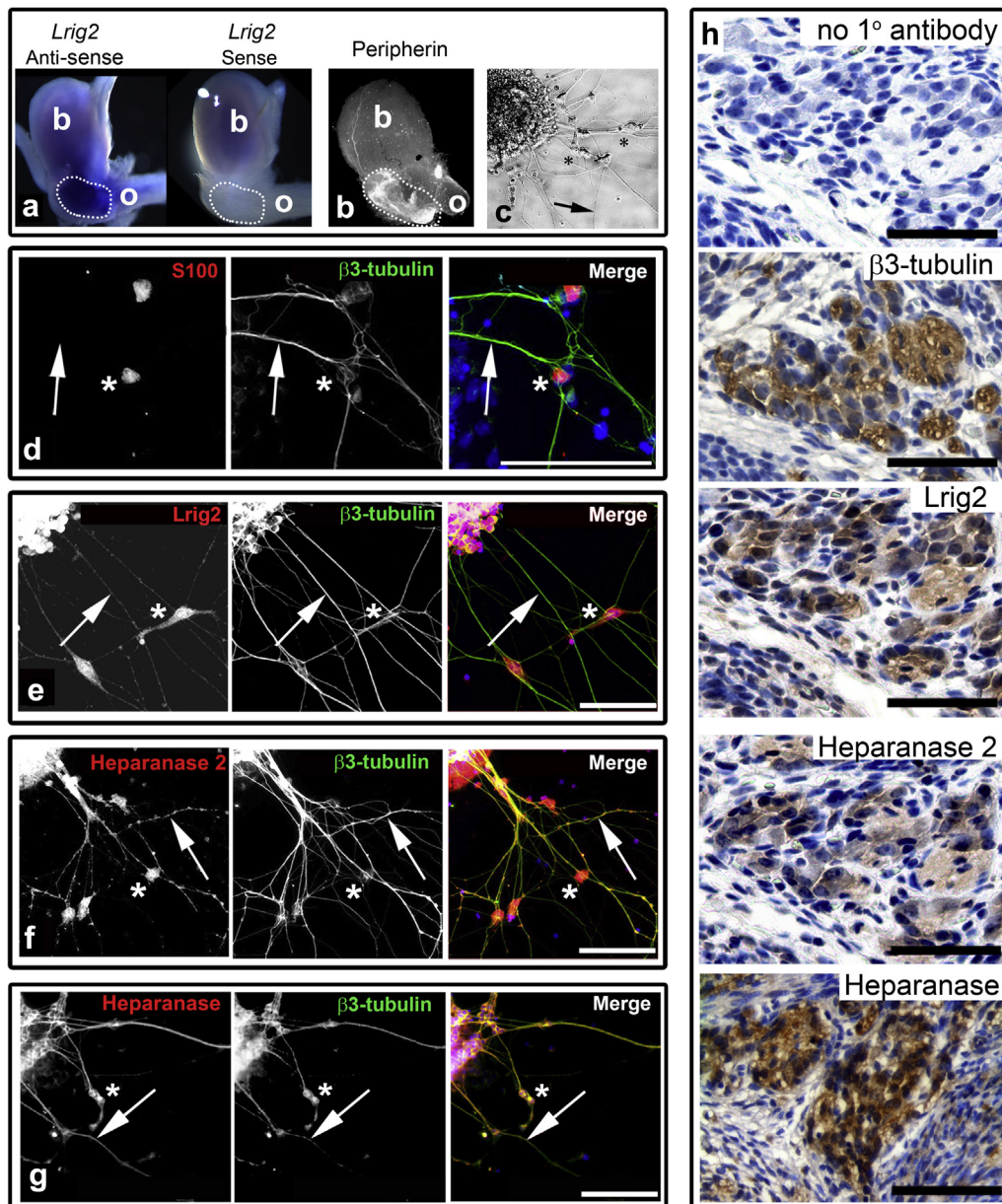


Figure 4 | Neuronal localization of leucine-rich repeats and Ig-like domains 2 (Lrig2) and heparanase 2. (a) Whole-mount *in situ* hybridization for *Lrig2*. Side views of embryonic day 15 wild-type bladders, with the left frame showing anti-sense probe and the right frame showing control sense probe. Note the strong signal (blue) at the junction of the body (b) and outflow (o) corresponding to the location of the pelvic ganglia (dotted outline). Blue color in the body is nonspecific trapping in the lumen in both genotypes. (b) Similar side view of whole-mount embryonic bladder immunostained for peripherin (white). The pelvic ganglion (dotted outline) is strongly positive. b, body; o, outflow. (c) Phase contrast of embryonic pelvic ganglion explant. After 1 day in culture, processes (arrow) had emerged from the cell mass (upper left of the frame), as had cell bodies (asterisks). (d–g) Immunocytochemistry of pelvic ganglia explants. The first 2 frames in each row show signals (white) for individual proteins (red or green) named in each frame. The final (merge) frame in each row shows double immunostaining, with nuclei stained with 4',6-diamidino-2-phenylindole (blue). (d) The glial marker, S100, was immunodetected in cell bodies (asterisks) that had emerged from the explanted mass, whereas emerged processes (arrows) immunostained for the neuronal microtubule protein β3-tubulin. (e) Emerged cell bodies (asterisks) and processes (arrows) immunostained for Lrig2. (f) Emerged cell bodies (asterisks) and neuronal processes (arrows) immunostained for heparanase 2. (g) Neuronal processes (arrows) immunostained for heparanase, the classical heparanase. Asterisks indicate the cell body. Bars in (d–g) = 100 μm. (h) Bright field immunohistochemistry of neonatal pelvic ganglion immunostained (brown) for β3-tubulin, Lrig2, heparanase 2, and the classical heparanase, with nuclei stained with hematoxylin. Note that all 3 antibodies label large cells: these are the cell bodies of autonomic neurons. Bar = 50 μm. To optimize viewing of this image, please see the online version of this article at www.kidney-international.org.

type or *Lrig2* mutant, are nearly always full at necropsy. In contrast, by 2 postnatal weeks, wild-type and *Lrig2* heterozygous necropsy bladders are usually empty, whereas bladders

of *Lrig2*^{−/−} mice usually contain urine. Therefore, a bladder emptying mechanism is becoming established in wild-type and heterozygous mice between birth and 2 weeks of age,

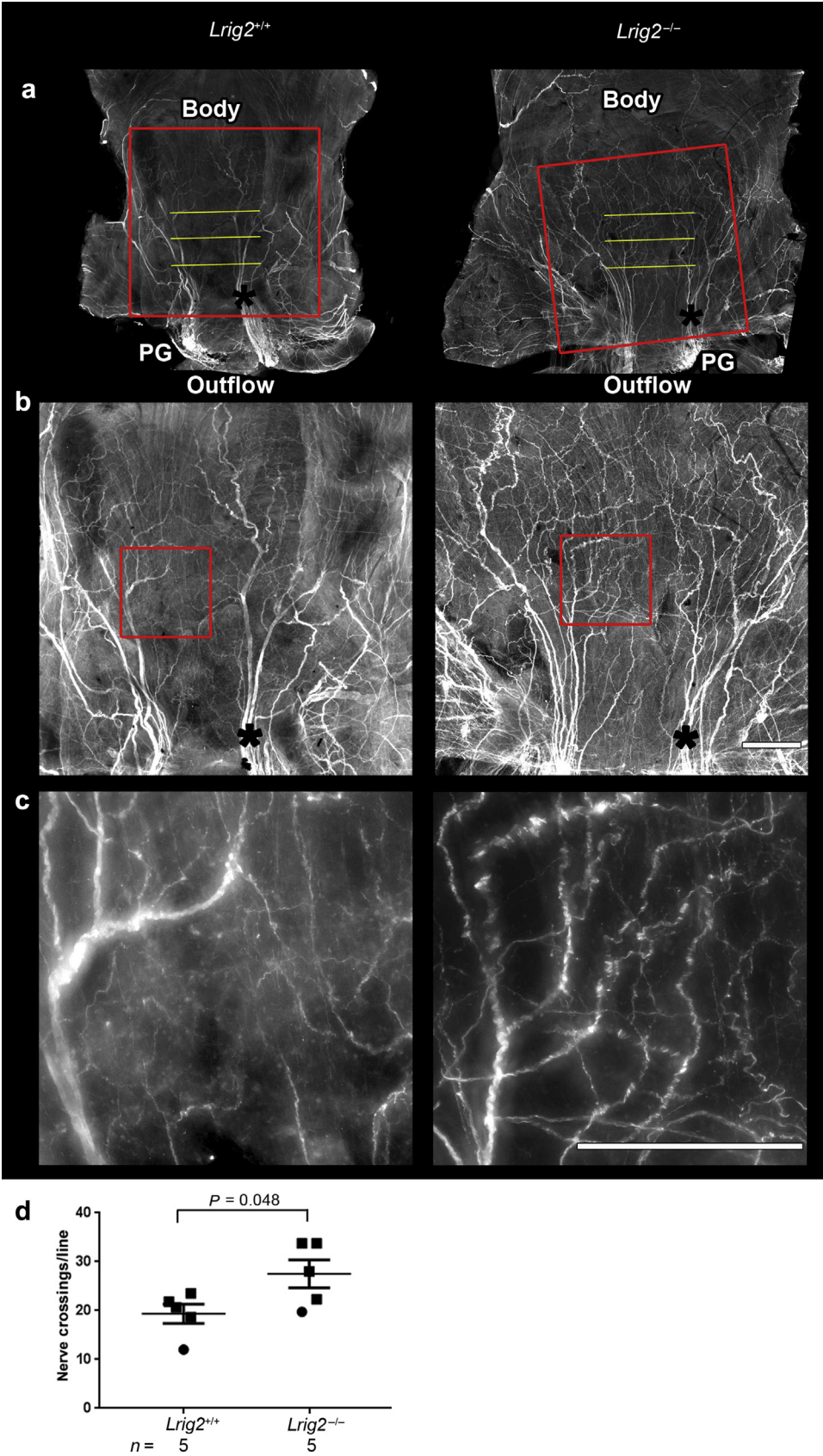


Figure 5 | Aberrant nerves in the leucine-rich repeats and Ig-like domains 2 (*Lrig2*)^{-/-} bladder body. (a) Whole wild-type (left column) and *Lrig2*^{-/-} (right column) bladder sheets immunostained for the neural protein peripherin. The top (cranial) part of (continued)

but this is defective in *Lrig2*^{-/-} mice. In older mice, *Lrig2*^{-/-} mutants urinated more frequently than did wild types but their individual voids were of lower volume. These dysfunctional patterns resemble those in people with UFS.⁵ *Lrig2*^{-/-} mouse urination defects were not caused by anatomic blockage of the outflow tract, consistent with functional bladder outflow obstruction. Urination patterns of *Lrig2* heterozygous mice appeared normal. Again, this finding is similar to that in human families affected by UFS because members who carry only one variant *LRIG2* allele are phenotypically normal.¹³ The fact that *Lrig2* heterozygous mice had normal urination despite containing markedly less *Lrig2* protein compared with wild-type bladders suggests that future treatments for UFS—for example, using gene therapy²⁸—may be effective if they produce only a modest amount of *Lrig2* protein. A previous report stated that another *Lrig2* homozygous mutant line²⁹ had normal bladder pressure as assessed by cystometry.¹² This mouse was created by random insertion of a gene trap into exon 11, resulting in fused *Lrig2* and β -galactosidase and neomycin resistance (*βgeo*), with a low level of *Lrig2* detectable in homozygous tissues.²⁹ Perhaps the different mode of targeting *Lrig2*, or background strain differences, account for the apparently discrepant bladder findings between this and the current study.

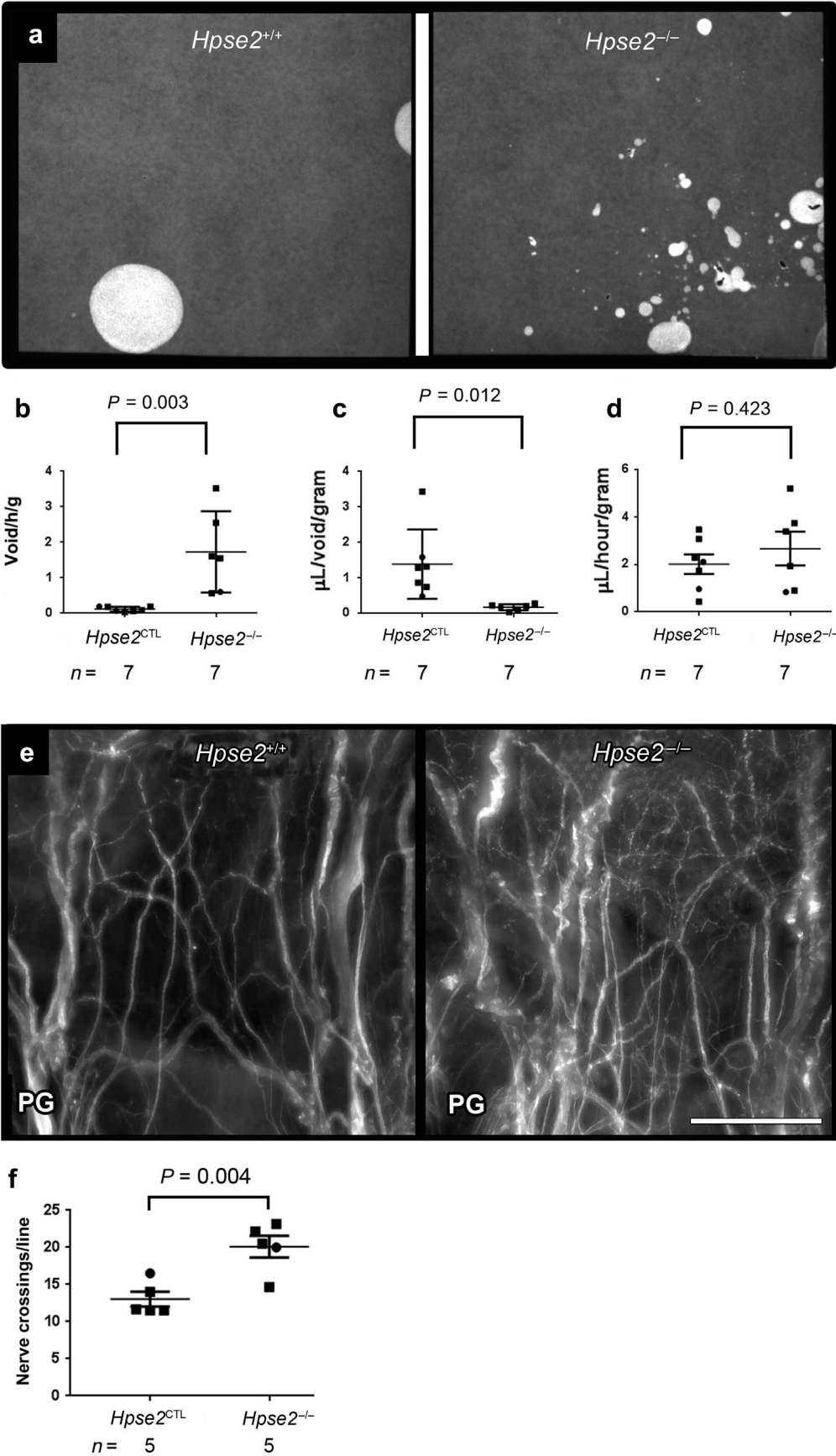
Mice homozygous for either *Lrig2* or *Hpse2* mutations had increased nerve density within the bladder body and decreased density around the outflow tract. *LRIG2*, heparanase 2, and heparanase itself were present in neural cells emanating from explanted embryonic pelvic ganglia and are present in intact pelvic ganglia. Our observations provide strong evidence that a peripheral neuropathy is part of the pathobiology of UFS bladder disease, whether caused by *HPSE2* or *LRIG2* variants. Figure 9 summarizes aberrations in the UFS bladder, linking established clinical observations with the new data.

Considering the UFS pathology, *Lrig2* and heparanase 2 also may be implicated peripherally in the facial nerve biology because persons with UFS have a characteristic grimace upon smiling.^{5,6} It had been hypothesized that a lesion affecting the pontine micturition center and the facial nerve nuclei, which control urination and facial expression, respectively, could account for the disparate phenotypes observed in the disease.⁵ However, the fact that the micturition center and the facial nerve nucleus are discrete structures makes a single lesion theory unlikely.³⁰ Further studies may resolve whether molecules mutated in UFS also play roles in the facial nerve and brainstem.

Lrig2 is implicated in vestibular and auditory nerve function,²⁹ and it modulates optic nerve regeneration.³¹ Another member of the *Lrig* family, *Lrig1*, acts as a break on primary dendrite formation and dendritic branching of hippocampal neurons.³² Heparanase, the enzyme inhibited by heparanase 2,¹¹ modulates neurite outgrowth from pheochromocytoma cells,³³ and heparanase protects against axonal degeneration after sciatic nerve injury.³⁴ Moreover, embryonic frogs depleted of heparanase 2 have disorganized peripheral nerves.³⁵ The current data showing aberrant nerves in *Hpse2* or *Lrig2* mutant bladders therefore add to a growing body of literature that the heparanase 2 and *Lrig* axis modulates neural biology. A biological explanation for the abnormal patterns of nerves in mutant and wild types is not yet clear. Our current study, however, detected no increased proliferation in cells within neonatal pelvic ganglia of *Lrig2* homozygous mutant mice versus wild types. We also found no significant differences in outgrowth of processes from explanted pelvic ganglia, comparing either *Hpse2* or *Lrig2* tissues with wild-type explants. One caveat is that it is not possible to know which neurites would have been destined to populate the bladder body or the outflow. The same applies to the nature of individual neuronal cell bodies visualized in pelvic ganglia histology. These considerations could be important because we counted more peripherin-positive nerves in the bladder body but fewer around the outlet. Bladders from adult *Lrig2*^{-/-} mutants were bulkier than those of control subjects, with prominent picosirius red staining upon histologic examination. Indeed, prominent lamina propria collagen was reported in *Hpse2* mutant bladders in their third postnatal week.¹² These changes may be secondary to bladder outlet obstruction.

Humans who have UFS associated with mutations of either *HPSE2* or *LRIG2* have similar bladder phenotypes,⁶ which is consistent with the hypotheses that the proteins encoded by these 2 genes maintain neural health by independent pathways or that the proteins interact, directly or indirectly, during their normal functions. Transheterozygote mice carrying one mutant allele at both the *Lrig2* and *Hpse2* loci did not have abnormal urination patterns, perhaps arguing against the idea that the encoded proteins directly interact. However, this observation also may be explained by a lack of haploinsufficient effects. It also should be noted that heparanase 2 may play biological roles in certain diseases unrelated to UFS, for example, in Alzheimer's disease³⁶ and head and neck cancer growth.³⁷ The same applies to *Lrig2* that has been implicated in tumor biology.^{15,16,19}

Figure 5 | (continued) the bladder is uppermost. Yellow lines denote regions in the bladder body where peripherin+ nerve crossings were quantified. Red boxes indicate regions magnified in the higher-power images, directly below. Black asterisks indicate the large bundles of nerves in the bladder body that connect with the pelvic ganglia (PG). (b,c) Higher magnifications showing large nerve bundles (asterisks) and finer fascicles in the bodies of the organs. Note the apparently more prominent peripherin+ structures in the *Lrig2*^{-/-} versus the wild-type littermate bladder. Bars = 200 μ m. (d) Quantification of peripherin+ structures (i.e., nerves crossing the yellow grid lines) showed a significant increase (average 40%) of nerves in *Lrig2*^{-/-} versus *Lrig2*^{+/+} bladders (mean \pm SEM, $P = 0.048$, 2-tailed unpaired Student t -test, $n = 5$). Male bladders are indicated by squares and female bladders by circles. To optimize viewing of this image, please see the online version of this article at www.kidney-international.org.



nNOS is a well-established mediator of smooth muscle relaxation, including in the lower urinary tract.³⁸ Indeed, *Nos1* homozygous mutant mice have incomplete bladder emptying caused by defective neurogenic relaxation of the outflow tract.⁴ We observed that the outflow tracts of mutant *Lrig2* or *Hpse2* bladders had a reduced number of nitrergic nerves compared with control subjects; if this finding translates to humans, the mouse observations could explain why the UFS bladder outflow fails to dilate, a key defect in the syndrome.⁵ We also documented an increased density of nerves in the bodies of bladders of mice with homozygous mutations of either *Lrig2* or *Hpse2*. The major nerve trunks within the normal murine bladder body contain cholinergic parasympathetic neurons that stimulate detrusor smooth muscle contraction.³ This feature may correlate with the detrusor overactivity typical of patients with UFS⁴ and that also is reported to be present in *Hpse2* homozygous mutant mice.¹² As with the long-term changes in the walls of *Lrig2*^{-/-} bladders, increased nerve density in the bladder body may be secondary to chronic outlet obstruction. On the other hand, loss of *Lrig2* can, in some circumstances, directly cause neuronal overgrowth, and *Lrig2* knockdown causes over-exuberant regeneration after optic nerve injury.³¹

We note that molecules involved in nerve biology are dysregulated in bladders of newborn *Lrig2* mutant mice. Upregulated transcripts included *Wnt family member 4*, encoding a growth factor implicated in establishing motor neurons³⁹ and neuromuscular junctions^{40,41}; *period circadian regulator 2*, encoding period circadian clock 2, implicated in micturition rhythm and expressed in bladders⁴²; and *shroom family member 1*, a member of a family implicated in central nervous system morphogenesis.⁴³ Apart from *Lrig2*, down-regulated transcripts included *G protein-coupled receptor 17*, encoding a leukotriene-responsive G protein-coupled receptor implicated in neural damage⁴⁴ and glial maturation⁴⁵; *capping actin protein of muscle Z-line subunit alpha 1*, encoding an F-actin-capping protein involved in neurite extension⁴⁶; *Wnt family member 2B* that maintains a neural progenitor state in retinal progenitors during embryogenesis⁴⁷; *contactin associated protein like 2*, encoding a presynaptic protein implicated in neuronal migration⁴⁸; and *SRY-box 10*, encoding a transcription factor expressed in neural crest progenitors and glia in autonomic ganglia.^{21,25,49} Further experiments are needed to define whether these molecules are functionally implicated in UFS. *Lrig2* binds neogenin, a receptor for

neuronal guidance molecules, and prevents neogenin shedding mediated by ADAM metallopeptidase domain 17-mediated proteolysis.³¹ Transcripts encoding neogenin and ADAM metallopeptidase domain 17 were unchanged in the *Lrig2*^{-/-} neonatal bladder transcriptome.

Biallelic putative null variants of *LRIG2* have been reported in a subset of families with UFS.¹³ Further emphasizing the role for *Lrig2* in bladder biology, this study discovered novel homozygous missense *LRIG2* variants in people with non-syndromic bladder outlet obstruction. The collective evidence we have presented suggests that each variant is likely to be pathogenic. In the future, proof of pathogenicity could be provided by finding dysfunctional bladders in mutant mice engineered to be homozygous for either variant. Neither patient had facial features of UFS, something also noted in a case report of a child¹³ with bladder disease harboring a homozygous *LRIG2* variant (c.2125C>T) resulting in a stop codon. Therefore, evidence exists that *LRIG2* variants occur in some persons with nonsyndromic bladder outlet obstruction. Conversely, we found no strong evidence that *LRIG2* variants are implicated in primary nonsyndromic VUR, and we reached a similar conclusions regarding *HPSE2* in this condition.¹⁰ Congenital bladder voiding dysfunction can be also caused by variants of *acta alpha 2*, *smooth muscle* encoding *alpha smooth muscle actin*,⁵⁰ *acta gamma 2*, *smooth muscle* encoding γ 2-actin,⁵¹ *cholinergic receptor muscarinic 3* encoding an acetylcholine receptor,⁵² *myosin heavy chain 11*, encoding myosin heavy chain 11,⁵³ and *myosin light chain kinase*, encoding a kinase involved in myosin activation.⁵⁴ Whether any of these are implicated in primary nonsyndromic VUR awaits investigation.

MATERIALS AND METHODS

Animals

Experiments were approved by the University of Manchester Biological Services Facility Committee and the United Kingdom Home Office (PPL 40/3550 and PAFFC1ffF), along with the Regional Ethics Committee of Umeå University (A193-12 and A1-2016). Experiments were conducted using Animal Research: Reporting of *In Vivo* Experiments best practice guidelines. *Hpse2* mutant mice studied here were created by gene-trap insertion into intron 6.¹⁰

Lrig2 mouse genotyping, VSOP, qRT-PCR, *in situ* hybridization, RNA sequencing, Western blot, whole bladder sheet processing, pelvic ganglia explants, and statistical analyses

See [Supplementary File](#).

Figure 6 | Urination defects and aberrant nerves in the bladder of heparanase 2 (*Hpse2*) mutant mice. (a) Voided stain on paper urination patterns produced by an *Hpse2*^{-/-} mouse (right frame) and a wild-type littermate (left frame). (b) Numbers of voids per unit time, with a significant ($P = 0.003$) increase in homozygous mutants versus control subjects. (c) Volumes of urine per void, with a significant ($P = 0.012$) decrease in homozygous mutants versus control subjects. (d) Total volumes of urine produced per unit time, with no significant ($P = 0.423$) difference between control (comprising wild-type and heterozygous mice) and *Hpse2*^{-/-} littermate pairs. Values in (b–d) are mean \pm SEM and are factored for weights of individual mice. Comparisons were made using 2-tailed unpaired Student *t*-tests. (e) Whole-mount immunostaining of 1-week postnatal bladders. Note increased peripherin+ (white) structures in the homozygous *Hpse2* mutant (right frame) versus the wild-type littermate (left frame) bladder. Bar = 200 μ m. (f) Quantification of peripherin+ structures (i.e., nerves crossing grid lines, as for [Figure 5a](#)) confirmed a significant ($P = 0.004$) increase in *Hpse2*^{-/-} versus control bladders. Data are mean \pm SEM, 2-tailed unpaired Student *t*-test, $n = 5$. Bars are 200 μ m. To optimize viewing of this image, please see the online version of this article at www.kidney-international.org.

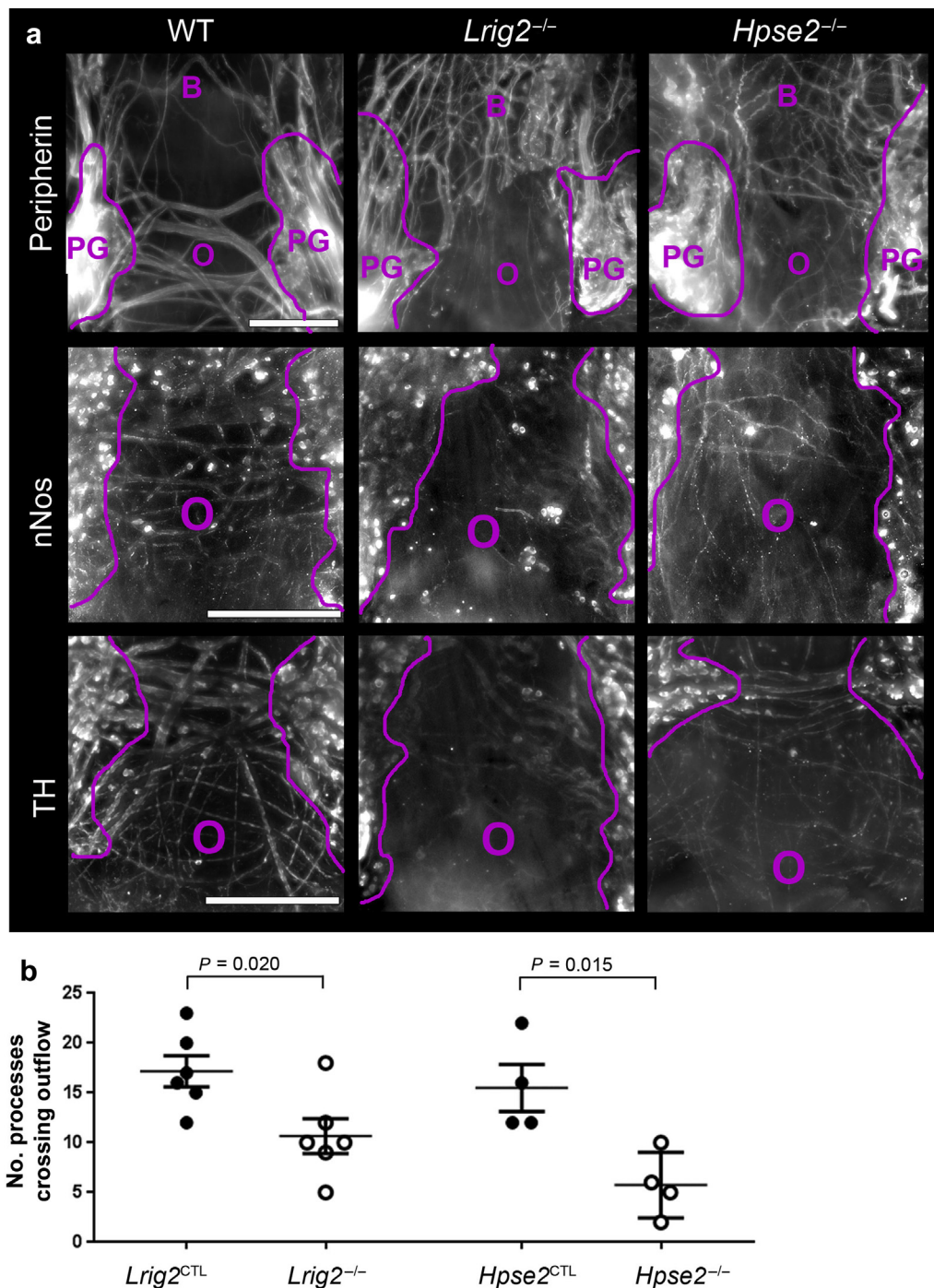


Figure 7 | Nerves around the bladder outflow tract. (a) Whole-mount immunostaining of bladders in the second week after birth. Bladders were reacted with antibodies to peripherin, a pan-neuronal marker (top row); neuronal nitric oxide synthase (nNOS), a marker of nitrergic parasympathetic neurons (middle row); or tyrosine hydroxylase (TH), a sympathetic neuron marker (bottom row). Purple lines define borders of pelvic ganglia (PG), and the bladder body is denoted by B and the outflow by O. Neurons spanning the 2 ganglia were detected in wild-type (WT) bladders (first column) with all 3 markers. Nerves in this zone were less prominent in both *Lrig2* (middle column) and *Hpse2* (right column) mutant outflow tracts. In contrast, in both the *Lrig2* and the *Hpse2* mutant bladders depicted, peripherin⁺ nerves in the bladder body were denser in each mutant than in the WT organ. Bars = 200 μ m. For peripherin immunostaining, 3 WT, 5 *Lrig2*^{-/-}, and 5 *Hpse2*^{-/-} mice were studied. For nNOS immunostaining, 3 WT, 4 *Lrig2*^{-/-}, and 5 *Hpse2*^{-/-} mice were studied. For TH immunostaining, 3 WT, 4 *Lrig2*^{-/-}, and 5 *Hpse2*^{-/-} mice were studied. (b) Quantification of peripherin-positive nerves around the outflow tracts. Note the significant reductions in both *Lrig2* and also *Hpse2* homozygous mutants compared with control mice. To optimize viewing of this image, please see the online version of this article at www.kidney-international.org.

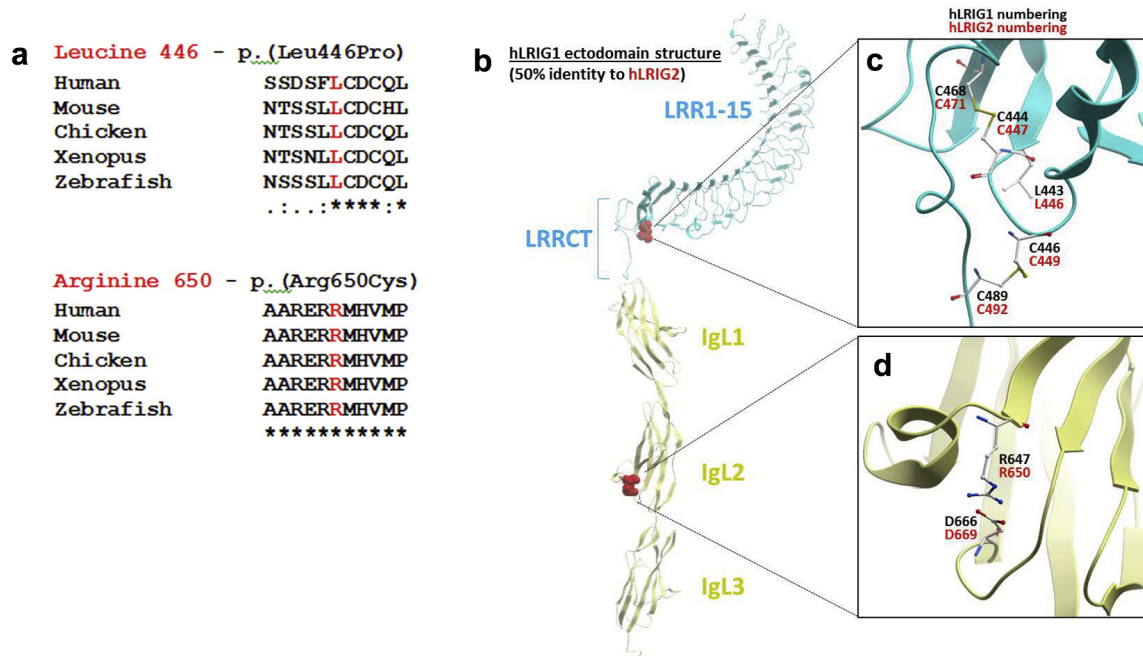


Figure 8 | Leucine-rich repeats and Ig-like domains 2 (LRIG2) missense variants. (a) Conservation of Leu446 and Arg650 between human, mouse, chicken, xenopus, and zebrafish protein sequences. An asterisk indicates positions which have a single, fully conserved residue; a colon indicates conservation between groups of strongly similar properties, scoring >0.5 in the Gonnet point accepted mutation 250 matrix; a period/full stop indicates conservation between groups of weakly similar properties, scoring <0.5 in the Gonnet point accepted mutation 250 matrix. (b) Extracellular domains of human LRIG1 (hLRIG1) that has approximately 50% sequence similarity to human LRIG2. Leucine-rich repeats (1–15) and Ig-like domains (1–3) are depicted. (c,d) These 2 frames show details of the regions containing the Leu446Pro (L446) and the Arg650Cys (R650) LRIG2 missense variants, respectively.

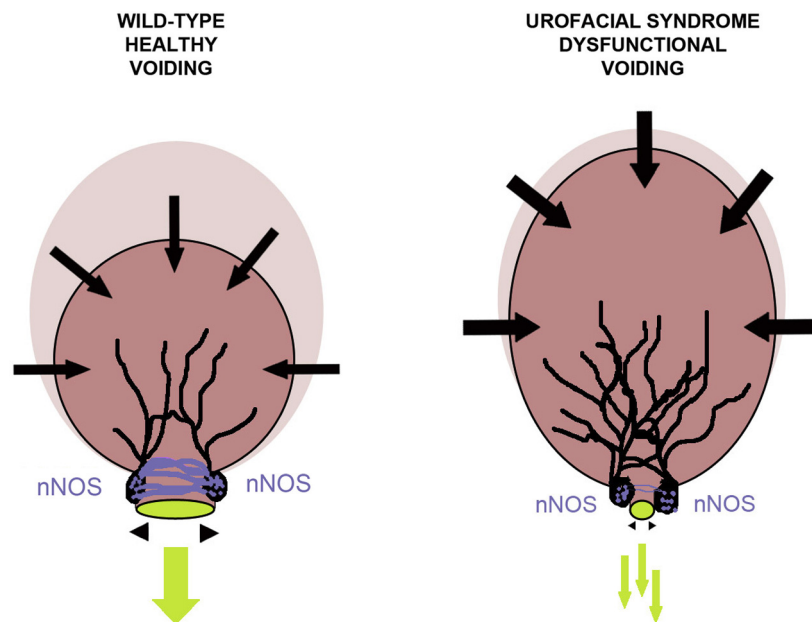


Figure 9 | Dysfunctional voiding in urofacial syndrome (UFS). In the healthy bladder (left) a robust urinary stream and efficient emptying are facilitated by full dilatation of the outflow tract–driven neuronal nitric oxide synthase (nNOS) nerves. In the UFS bladder (right) the stream is poor because the outflow fails to fully dilate, which is associated with downregulated nNOS. The detrusor muscle in the body of the UFS bladder is overactive, which is associated with an abundance of nerves in the body of the organ. Contractile forces in the bladder body are shown by black arrows facing inward, and outlet dilatation is shown by black arrowheads facing outward. Nitric oxide (nNOS) autonomic nerves around the outflow are depicted in purple, and those in the body (presumed cholinergic) are depicted in black. Urine is depicted in light green. The body of the uncontracted bladder is represented in lilac, and the voiding bladder body is shown in pink.

Human analyses

Informed consent or assent was obtained from subjects or their parents. Studies were approved by institutional ethics committees (University of Manchester [06138] and National Health Service [06/Q1406/52 and 11/NW/0021]). United Kingdom VUR DNA samples were collected under National Research Ethics Service number MREC/01/6/15, with the clinical cohort previously published.^{26,55} The 4C study of children with chronic renal failure has been described (<http://www.4c-study.org/>). *LRIG2* was analyzed using Sanger sequencing.

DISCLOSURE

All the authors declared no competing interests.

ACKNOWLEDGMENTS

We acknowledge technical support from Peter Walker and Grace Bako, University of Manchester Histology Core Facility, for help with histology; Ping Wang and Andy Hayes, University of Manchester Bioinformatics and Genomic Technologies Core Facilities, for undertraining RNA sequencing; David Spiller, University of Manchester Systems Microscopy Core Facility, for help with whole bladder imaging; Annika Holmberg, Charlotte Nordström, and Yvonne Jonsson, University of Umeå, for initial mouse colony investigation and Western blot analyses; and the staff at the Manchester Biological Services Facility. We acknowledge grant support from the Medical Research Council MR/L002744/1 (ASW, ENH, NJG, WGN); Horizon 2020 Marie Skłodowska-Curie Actions Initial Training Network (942937) RENALTRACT (ASW, NJG, FL); Newlife Foundation (ASW, WGN, ENH); NIHR Academic Lecturer scheme (HMS); Academy of Medical Sciences (HMS); Kidneys for Life pump priming project (ASW); Kidney Research UK Non-Clinical Training Fellowship scheme (NAR); the Wellcome Trust Functional Genomics Programme Grant 066647 (ASW); the Swedish Cancer Society, contract 160618 (HH and RH); and the Cancer Research Foundation in Northern Sweden, AMP13-721 (HH and RH). Histology Core Facility equipment was purchased with grants from the University of Manchester Strategic Fund. We acknowledge provision of genetics samples from the United Kingdom VUR Study Group comprising Beattie J, Bradbury M, Coad N, Coulthard M, Cuckow P, Dossetor J, Dudley J, Hughes D, Feather SA, Fitzpatrick M, Goodship JA, Goodship TH, Griffin N, Gullett AM, Haycock G, Hodes D, Houtman P, Hughes A, Hulton S, Hunter E, Iqbal J, Inward C, Jackson J, Jadresic L, Jaswon M, Jones C, Jones R, Judd B, Kier M, Kilby A, Lambert H, Lewis M, Malcolm S, Marks S, Maxwell H, McGraw M, Milford D, Moghal N, O'Connor M, O'Donoghue DJ, Ognanovic M, Plant N, Postlethwaite R, Rees L, Reid C, Rfidah E, Rigden S, Sandford R, Savage M, Sayer JA, Scanlan J, Sinha S, Stephens S, Stewart A, Storr J, Taheri S, Taylor CM, Tizard J, Trompeter R, Tullus K, Verber I, Van't Hoff W, Vernon S, Verrier-Jones K, Watson A, Webb N, Wilcox D, and Woolf AS; and from the 4C Study Group, comprising Aksu N, Alpaly A, Anarat A, Arbeiter K, Ardissino GL, Balat A, Baskin E, Bayazit A, Büscher R, Cakar N, Caldas Afonso A, Caliskan S, Candan C, Canpolat N, Donmez O, Doyon A, Drozd D, Dusek J, Duzova A, Emre S, Erdogan H, Feldkötter M, Fischbach M, Galiano G, Haffner D, Harambat J, Jankauskiene A, Jeck N, John U, Jungraithmair T, Kemper M, Kiyak A, Kracht D, Kranz B, Laube G, Litwin M, Matteucci CM, Montini G, Melk A, Mir S, Niemirska A, Peco-Antic A, Ozcelik G, Pelan E, Picca S, Pohl M, Querfeld U, Ranchin B, Schaefer F, Shroff R, Simonetti G, Sözeri B, Soylemezoglu O, Tabel Y, Testa S, Trivelli A, Vidal E, Wigger M, Wühl E, Wygoda S, Yalcinkaya F, Yilmaz E, Zeller R, and Zurowska AM.

SUPPLEMENTARY MATERIAL

Supplementary Results. Modeling effects of *leucine-rich repeats* and *Ig-like domains 2* variants.

Supplementary Methods.

Supplementary References.

Figure S1. Neonatal and 2-week urinary bladder histology. (A–F) Bladder outflow: 5- μ m paraffin sections cut transversely across the outflow comparing wild-type with *leucine-rich repeats* and *Ig-like domains 2* (*Lrig2*)^{−/−} mutants at neonatal, 2-week, and adult stages. All had patent outflow tracts. Bars = 100 μ m. (G–L) Bladder body: 2-week bladder sections were reacted with Masson's trichrome (G and H; muscle and urothelium = red and collagen = light blue), or muscle immunostained (brown) for α -smooth muscle actin (I,J), or urothelium immunostained (brown) for uroplakin II (K,L). Note that staining patterns were similar in *Lrig2*^{−/−} and *Lrig2*^{+/+} bladders. Bars = 50 μ m.

Figure S2. Ki67 immunostaining of adult bladders. All sections were counterstained with hematoxylin. Panels show high-power views of detrusor, lamina propria, and urothelial layers in wild types and mutants. Selections of nuclei positive for Ki67 are indicated by arrows. Bars are 50 = μ m.

Figure S3. Immunostaining of neonatal pelvic ganglia. (A) Immunohistochemistry for Wnt family member 4 (Wnt4) and capping actin protein of muscle Z-line subunit alpha 1 (Capza1), encoded by 2 transcripts highlighted in unsupervised hierarchical clustering (Figure 3) and neuronal nitric oxide synthase (nNOS), showed that all 3 were detectable in wild-type neonatal pelvic ganglia. The bottom left frame is a negative control with no primary antibody. All sections were counterstained with hematoxylin, with positive immunohistochemical signal in brown. (B) Quantification of nNOS immunohistochemical signals in neonatal ganglia showed a small but statistically significant reduction (Student *t*-test, *P* = 0.014) in *leucine-rich repeats* and *Ig-like domains 2* (*Lrig2*)^{−/−} tissues (mean \pm SEM in 5 control subjects = 48.4 \pm 10.7 arbitrary units and in 5 mutants = 40.5 \pm 10.4). nNOS immunostaining was semi-quantified by taking the average pixel intensity reading for the pelvic ganglia region only in ImageJ.

Figure S4. Quantitative reverse transcription–polymerase chain reaction for *nitric oxide synthase 1* (*Nos1*) in neonatal bladders and attached outflow tracts. For both *leucine-rich repeats* and *Ig-like domains 2* (*Lrig2*) homozygous mutant tissues and the *heparanase 2* (*Hpse2*) mutant tissues, *Nos1* transcripts levels were reduced compared with littermate control subjects. Values are shown as mean \pm SEM, with the value for the mean of each wild-type group defined as “1.”

Figure S5. Quantification of processes emanated from pelvic ganglia explants. Fragments of embryonic pelvic ganglia were explanted and the numbers of processes that had emanated from them were counted after 1 day in culture. Results are shown as median and ranges, with values factored for the length of the perimeter in each explant. The wild-type median was defined as “1.” There were no significant differences (all *P* > 0.05) between wild-type explants and either *leucine-rich repeats* and *Ig-like domains 2* (*Lrig2*) or *heparanase 2* (*Hpse2*) mutants as assessed by Kruskal–Wallis tests. The number of ganglia assessed are shown in the figure.

Figure S6. Western blot quantification of *Lrig2* protein levels in bladder lysates. Total protein was extracted from wild-type, *Lrig2* heterozygous, and *Lrig2* homozygous mutant mouse bladders and 35 μ g resolved on a polyacrylamide gel. Each lane represents a separate bladder sample, with genotypes loaded at random. Wild-type *Lrig2* is indicated by the black arrow, at 125 kDa. The red box indicates an example of wild-type, heterozygous, and homozygous bladder samples, with strong, low, and absent *Lrig2* bands, respectively. Supplementary material is linked to the online version of the paper at www.kidney-international.org.

REFERENCES

- Mendell JR, Al-Zaidy S, Shell R, et al. Single-dose gene-replacement therapy for spinal muscular atrophy. *N Engl J Med*. 2017;377:1713–1722.

2. Benarroch EE. Neural control of the bladder: recent advances and neurologic implications. *Neurology*. 2010;75:1839–1846.
3. Keast JR, Smith-Anttila CJ, Osborne PB. Developing a functional urinary bladder: a neuronal context. *Front Cell Dev Biol*. 2015;3:53.
4. Burnett AL, Calvin DC, Chamness SL, et al. Urinary bladder-urethral sphincter dysfunction in mice with targeted disruption of neuronal nitric oxide synthase models idiopathic voiding disorders in humans. *Nat Med*. 1997;3:571–574.
5. Ochoa B. Can a congenital dysfunctional bladder be diagnosed from a smile? The Ochoa syndrome updated. *Pediatr Nephrol*. 2004;19:6–12.
6. Newman WG, Woolf AS. Urofacial syndrome. GeneReviews. <https://www.ncbi.nlm.nih.gov/books/NBK154138/>. Published August 22, 2013; updated June 7, 2018.
7. Roberts NA, Hilton EN, Woolf AS. From gene discovery to new biological mechanisms: heparanases and congenital urinary bladder disease. *Nephrol Dial Transplant*. 2016;31:534–540.
8. Daly SB, Urquhart JE, Hilton E, et al. Mutations in HPSE2 cause urofacial syndrome. *Am J Hum Genet*. 2015;96:963–969.
9. Pang J, Zhang S, Yang P, et al. Loss-of-function mutations in HPSE2 cause the autosomal recessive urofacial syndrome. *Am J Hum Genet*. 2010;86:957–962.
10. Stuart HM, Roberts NA, Hilton EN, et al. Urinary tract effects of HPSE2 mutations. *J Am Soc Nephrol*. 2015;26:797–804.
11. Levy-Adam F, Feld S, Cohen-Kaplan V, et al. Heparanase 2 interacts with heparan sulfate with high affinity and inhibits heparanase activity. *J Biol Chem*. 2010;285:28010–28019.
12. Guo C, Kaneko S, Sun Y, et al. A mouse model of urofacial syndrome with dysfunctional urination. *Hum Mol Genet*. 2015;24:1991–1999.
13. Stuart HM, Roberts NA, Burgu B, et al. LRIG2 mutations cause urofacial syndrome. *Am J Hum Genet*. 2013;92:259–264.
14. Fadda A, Butt F, Tomei S, et al. Two hits in one: whole genome sequencing unveils LIG4 syndrome and urofacial syndrome in a case report of a child with complex phenotype. *BMC Med Genet*. 2016;17:84.
15. Lindquist D, Kvarnbrink S, Henriksson R, Hedman H. LRIG and cancer prognosis. *Acta Oncol*. 2014;53:1135–1142.
16. Simion C, Cedano-Prieto ME, Sweeney C. The LRIG family: enigmatic regulators of growth factor receptor signaling. *Endocr Relat Cancer*. 2014;21:R431–R443.
17. Wong VW, Stange DE, Page ME, et al. Lrig1 controls intestinal stem-cell homeostasis by negative regulation of ErbB signalling. *Nat Cell Biol*. 2012;14:401–408.
18. Abaira VE, Satoh T, Fekete DM, Goodrich LV. Vertebrate Lrig3-ErbB interactions occur in vitro but are unlikely to play a role in Lrig3-dependent inner ear morphogenesis. *PLoS One*. 2010;5:e8981.
19. Rondahl V, Holmlund C, Karlsson T, et al. Lrig2-deficient mice are protected against PDGFB-induced glioma. *PLoS One*. 2013;8:e73635.
20. Sugino Y, Kanematsu A, Hayashi Y, et al. Voided stain on paper method for analysis of mouse urination. *Neurol Urodyn*. 2008;27:548–552.
21. Wiese CB, Ireland S, Fleming NL, et al. A genome-wide screen to identify transcription factors expressed in pelvic ganglia of the lower urinary tract. *Front Neurosci*. 2012;6:130.
22. Wiese CB, Deal KK, Ireland SJ, et al. Migration pathways of sacral neural crest during development of lower urogenital tract innervation. *Dev Biol*. 2017;429:356–369.
23. Stewart AL, Anderson RB, Kobayashi K, et al. Effects of NGF, NT-3 and GDNF family members on neurite outgrowth and migration from pelvic ganglia from embryonic and newborn mice. *BMC Dev Biol*. 2008;8:73.
24. Cheng S, Yang X, Zhang Y, Xiao C. Culture of major pelvic ganglion neurons from adult rat. *Cytotechnology*. 2013;65:663–669.
25. Hao MM, Capoccia E, Cirillo C, et al. Arundic acid prevents developmental upregulation of S100B expression and inhibits enteric glial development. *Front Cell Neurosci*. 2017;11:42.
26. Cordell HJ, Darlay R, Charoen P, et al. Whole-genome linkage and association scan in primary, nonsyndromic vesicoureteric reflux. *J Am Soc Nephrol*. 2010;21:113–123.
27. Danzer E, Kiddoo DA, Redden RA, et al. Structural and functional characterization of bladder smooth muscle in fetal rats with retinoic acid-induced myelomeningocele. *Am J Physiol Renal Physiol*. 2007;292:F197–F206.
28. Buckinx R, Van Remoortel S, Gijssels R, et al. Proof-of-concept: neonatal intravenous injection of adeno-associated virus vectors results in successful transduction of myenteric and submucosal neurons in the mouse small and large intestine. *Neurogastroenterol Motil*. 2016;28:299–305.
29. Del Rio T, Nishitani AM, Yu WM, et al. In vivo analysis of Lrig genes reveals redundant and independent functions in the inner ear. *PLoS Genet*. 2013;9:e1003824.
30. Ganesan I, Thomas T. More than meets the smile: facial muscle expression in children with Ochoa syndrome. *Med J Malaysia*. 2011;66:507–509.
31. van Erp S, van den Heuvel DMA, Fujita Y, et al. Lrig2 negatively regulates ectodomain shedding of axon guidance receptors by ADAM proteases. *Dev Cell*. 2015;35:537–552.
32. Alsina FC, Hita FJ, Fontanet PA, et al. Lrig1 is a cell-intrinsic modulator of hippocampal dendrite complexity and BDNF signaling. *EMBO Rep*. 2016;17:601–616.
33. Cui H, Shao C, Liu Q, et al. Heparanase enhances nerve-growth-factor-induced PC12 cell neurogenesis via the p38 MAPK pathway. *Biochem J*. 2011;440:273–282.
34. Whitehead MJ, McGonigal R, Willison HJ, et al. Heparanase attenuates axon degeneration following sciatic nerve transection. *Sci Rep*. 2018;8:5219.
35. Roberts NA, Woolf AS, Stuart HM, et al. Heparanase 2, mutated in urofacial syndrome, mediates peripheral neural development in *Xenopus*. *Hum Mol Genet*. 2014;23:4302–4314.
36. García B, Martín C, García-Suárez O, et al. Upregulated expression of heparanase and heparanase 2 in the brains of Alzheimer's disease. *J Alzheimers Dis*. 2017;58:185–192.
37. Gross-Cohen M, Feld S, Doweck I, et al. Heparanase 2 attenuates head and neck tumor vascularity and growth. *Cancer Res*. 2016;76:2791–2801.
38. Andersson KE, Persson K. Nitric oxide synthase and the lower urinary tract: possible implications for physiology and pathophysiology. *Scand J Urol Nephrol Suppl*. 1995;175:43–53.
39. Agalliu D, Takada S, Agalliu I, et al. Motor neurons with axial muscle projections specified by Wnt4/5 signaling. *Neuron*. 2009;61:708–720.
40. Inaki M, Yoshikawa S, Thomas JB, et al. Wnt4 is a local repulsive cue that determines synaptic target specificity. *Curr Biol*. 2007;17:1574–1579.
41. Strohlic L, Falk J, Goillot E, et al. Wnt4 participates in the formation of vertebrate neuromuscular junction. *PLoS One*. 2012;7:e29976.
42. Wu C, Sui G, Archer SN, et al. Local receptors as novel regulators for peripheral clock expression. *FASEB J*. 2014;28:4610–4616.
43. Hagens O, Ballabio A, Kalscheuer V, et al. A new standard nomenclature for proteins related to Apx and Shroom. *BMC Cell Biol*. 2006;7:18.
44. Marucci G, Dal Ben D, Lambertucci C, et al. The G protein-coupled receptor GPR17: overview and update. *ChemMedChem*. 2016;11:2567–2574.
45. Viganò F, Schneider S, Cimino M, et al. GPR17 expressing NG2-glia: oligodendrocyte progenitors serving as a reserve pool after injury. *Glia*. 2016;94:287–299.
46. Davis DA, Wilson MH, Giraud J, et al. Capzb2 interacts with beta-tubulin to regulate growth cone morphology and neurite outgrowth. *PLoS Biol*. 2009;7:e1000208.
47. Kubo F, Takeichi M, Nakagawa S. Wnt2b inhibits differentiation of retinal progenitor cells in the absence of Notch activity by downregulating the expression of proneural genes. *Development*. 2005;132:2759–2770.
48. Peñaarriano O, Abrahams BS, Herman EI, et al. Absence of CNTNAP2 leads to epilepsy, neuronal migration abnormalities, and core autism-related deficits. *Cell*. 2011;147:235–246.
49. Boesmans W, Lasrado R, Vanden Berghe P, et al. Heterogeneity and phenotypic plasticity of glial cells in the mammalian enteric nervous system. *Glia*. 2015;63:229–241.
50. Richer J, Milewicz DM, Gow R, et al. R179H mutation in ACTA2 expanding the phenotype to include prune-belly sequence and skin manifestations. *Am J Med Genet A*. 2012;158A:664–668.
51. Thorson W, Diaz-Horta O, Foster J 2nd, et al. De novo ACTG2 mutations cause congenital distended bladder, microcolon, and intestinal hypoperistalsis. *Hum Genet*. 2014;133:737–742.
52. Weber S, Thiele H, Mir S, et al. Muscarinic acetylcholine receptor M3 mutation causes urinary bladder disease and a prune-belly-like syndrome. *Am J Hum Genet*. 2011;89:668–674.
53. Gauthier J, Ouled Amar Bencheikh B, Hamdan FF, et al. A homozygous loss-of-function variant in MYH11 in a case with megacystis-microcolon-intestinal hypoperistalsis syndrome. *Eur J Hum Genet*. 2015;23:1266–1268.
54. Halim D, Brosens E, Muller F, et al. Loss-of-function variants in MYLK cause recessive megacystis microcolon intestinal hypoperistalsis syndrome. *Am J Hum Genet*. 2017;101:123–129.
55. Lambert HJ, Stewart A, Gullett AM, et al. Primary, non-syndromic vesicoureteric reflux and nephropathy in sibling pairs: a United Kingdom cohort for a DNA bank. *Clin J Am Soc Nephrol*. 2011;6:760–766.